Proceedings of Science and Mathematics
Faculty of Science, Universiti Teknologi Malaysia
Vol. 23, 2024, page 51-59

Mathematical Modelling of Harmful Algal Blooms

Santun Syafitri Mulyadi, Fatin Nadiah Mohamed Yussof
Department of Mathematics, Universiti Teknologi Malaysia
Corresponding author: fatinnadiah@utm.my

Abstract
An algal bloom is a condition where the excessive growth of algae, produce toxins and becoming harmful when it causes damaging effects. This study investigates a mathematical model of plankton-nutrient interaction, analyze the stability of equilibrium points, examine the oscillation properties, and investigate the effect of environmental carrying capacity on the HAB model. This research proposes a mathematical model of HAB dynamics consists of phytoplankton and zooplankton to describe the interaction between phytoplankton and zooplankton, examining three equilibrium point. The stability of equilibrium points is analyzed, revealing both stable and unstable. The instability may be due to disruptions in both populations, while the stability exists when the populations converge to 0. The oscillation properties of the model show that phytoplankton initially grow, then drop due to resource depletion, reducing zooplankton predation and allowing phytoplankton recovery. Zooplankton populations decreases due to toxins from phytoplankton. To study equilibrium stability, the environmental carrying capacity (K) is u sed. As K increases, the system become stable up to a specific value. Beyond this, it becomes unstable changing to a neutral saddle equilibrium and no further bifurcations occur. Recommendations for future studies include investigating non-toxin phytoplankton and nutrient interactions, incorporating discrete-time delays, exploring other delays that could influence the stability, and investigate factors affecting HAB occurrence.
Keywords: Harmful Algal Bloom; Phytoplankton; Zooplankton; equilibrium points

1. Introduction

Harmful Algal Bloom (HAB) is an annual phenomenon that is harmful to animals, human and economic sectors [1],[2]. Economic effects include the wreckage of tourism attraction spots, since activities such as fishing and snorkelling cannot be carried out [3]. HAB happened due to excessive growth of algae in oceans, lakes, or rivers and it occurs when certain types of algae receive many nutrients from agricultural runoff or sewage discharge.

The first recorded occurrence of HAB in Malaysia was in 1976 [4] and it has been observed in many locations such as Tumpat, Kelantan [5], Sepanggar Bay off Kota Kinabalu, Sabah [6], and Tanjung Kupang, Johor [3]. Nutrient pollution, including increased levels of phosphorus and nitrogen, is a factor to the occurrence of HABs [7].

Phytoplankton are tiny, and photosynthetic organisms that float in water. Some types of phytoplankton can grow quickly which then can form dense concentrations or “blooms”. From [2], the main contributors to HAB are diatoms and dinoflagellate but there are also few other types which are cyanobacteria, green algae, and coccolithophore [8] and these usually referred as toxic phytoplankton (TPP). Apart from that, zooplankton also important in HAB formation. They are usually heterotrophic, meaning they feed on other organisms. [9] mentioned that some zooplankton such as Daphnia can interact with toxic cyanobacteria like Microcystis, which can affect the dynamics of HAB and can influence the sensitivity of zooplankton to toxins produced by harmful algae.

This research aims to (1) examine a mathematical model of plankton interaction (2) analyze the stability of equilibrium point and the oscillation properties of the system (3) investigate the effect of environmental carrying capacity on HAB model.

2. Literature Review

2.1 Harmful Algal Bloom

Harmful algal blooms (HABs) are very risky to human health mainly through the production of toxins by few species of algae. These toxins can enter the food chain through polluted shellfish, leading to various forms of shellfish poisoning if consumed. A massive algal bloom can also lead to oxygen depletion in the water, a phenomenon known as hypoxia, which can result in the mortality of aquatic life such as fish and shrimp. HAB can be recognized from the color of the water. Combination of organisms can color the water giving rise to red, mahogany, brown, and green tides [10]. These blooms can present a variety of colors due to the types of algae involved and the specific pigments they produce. For instance, green blooms are often caused by cyanobacteria such as Microcystis or Anabaena which will make the water become a bright green [11]. Red tides occur in coastal marine environments are caused by dinoflagellates. These blooms can change from reddish brown due to the pigment fucocanthin.

The occurrence of HAB has been observed in many countries globally. [12] documented blooms occurring in Indonesia during April 2004 and May 2005. These incidents were observed in three coastal bays: Jakarta Bay, Lampung Bay, and Ambon Bay. A massive fish killing were reportedly happened during that time due to the lack of dissolved oxygen caused breathing difficulties for the fish. The toxins from HAB can lead to various types of illnesses such as shellfish poisoning. For example, six persons were reported hospitalized due to paralytic shellfish poisoning (PSP) that happened in Tumpat, Kelantan [5]. Some HAB toxins also have neurotoxic effects that can lead to symptoms such as confusion, dizziness, headaches, and in severe cases, seizures [13].

2.2 Prey-Predator Model

The prey-predator model usually consists of differential equations that describe the interactions between prey and predator populations over time [14]. This formulation involves a pair of non-linear first order differential equation (ODE), serving as prey-predator model to show the interaction of two species in a biological system. For example, the Lotka-Volterra model, has been widely used to understand the dynamics of prey-predator interactions [15]. The general form of the Lotka-Volterra model is represented by the following equation:

$$\begin{aligned} \frac{dx}{dt} &= \alpha x - \beta xy, \\ \frac{dy}{dt} &= \delta xy - \gamma y \end{aligned} \tag{1}$$

where x is the population of the prey species, y is the population of the predator species, α is the intrinsic growth rate of the prey population, β is the predation rate coefficient, δ is the rate at which the predator population increases per prey consumed and γ is the death rate at the predator population.

In the context of the formulation of HABs model, it has been assumed that the growth of phytoplankton population follows the logistic law with intrinsic growth rate '*r*' and environmental carrying capacity '*K*'. As mentioned previously, some phytoplankton release toxic substances and hence reduce the growth of zooplankton by decreasing the grazing pressure. Zooplankton grazing plays an important role in the initial stages of outbreaks. Keeping these properties of phytoplankton-zooplankton population in mind, two types of predational forms have been assumed: simple law of mass action and Holling-type response term [16]. When phytoplankton populations do not produce toxin, the predation rate will follow the simple law of mass action and in this case, zooplankton eating is proportional to the phytoplankton density and thus limiting the production of the phytoplankton. But, as liberation of toxin reduces the growth of zooplankton, causes substantial mortality of zooplankton and in this period, phytoplankton population is not easily available. Hence, a more common and obvious choice is of the Holing type II functional form to describe the grazing phenomena in the presence of toxic substances. From the above assumptions, the following differential equations can be formed:

$$\frac{dP}{dt} = rP\left(1 - \frac{P}{K}\right) - \alpha PZ,$$
$$\frac{dZ}{dt} = \beta PZ - \mu Z - \frac{\theta PZ}{\gamma + P}. \quad (2)$$

Here, P and Z represent the density of phytoplankton and zooplankton population, respectively, $\alpha(>0)$ is the specific predation rate and $\beta(>0)$ represents the ratio of biomass consumed by zooplankton for its growth. $\mu(>0)$ is the mortality rate of zooplankton, $\theta(>0)$ is the rate of toxin production per phytoplankton and $\gamma(>0)$ is the half saturation constant. r is the growth rate of TPP and K is the environmental carrying capacity.

Equation (2) can be used to study the dynamics of ecological system where prey and predator interactions are significant. It helps in understanding the limit cycles, stability, and the impact of various parameters on the ecosystem.

3. Methodology

3.1 Ordinary Differential Equation (ODE)

In this part, the minimal mathematical background required to analyze the ODE in the survey. The behavior of solutions of the autonomous system is discussed near an isolated critical point (x_0, y_0) where $f(x_0, y_0) = g(x_0, y_0) = 0$.

$$\frac{dx}{dt} = f(x, y),$$
$$\frac{dy}{dt} = g(x, y) \quad (3)$$

If the neighbourhood point does not has any critical point, the point is called isolated. The function of f and g are assumed as continuously differentiable in (x_0, y_0) neighbourhood. Assumption of $x_0 = y_0 = 0$ is made without loss of generality. Otherwise, substitutions are made for $u = x - x_0, v = y - y_0$. Hence, $\frac{dx}{dt} = \frac{du}{dt}$ and $\frac{dy}{dt} = \frac{dv}{dt}$. The system is equivalent to

$$\frac{du}{dt} = f(u + x_0, v + y_0) = f_1(u, v)$$
$$\frac{dv}{dt} = g(u + x_0, v + y_0) = g_1(u, v) \quad (3)$$

where the isolated critical value is $(0,0)$.

3.2 Equilibrium Point

An equilibrium point is a point which the system is stable by examining the eigenvalues. In the context of HAB, equilibrium point is important for accessing system stability. Three types of equilibrium points are examined in order to identify the stability (1) a trivial equilibrium point (2) an axial equilibrium and (3) the interior equilibrium.

3.3 Stability of Linear Systems

The eigenvalue-eigenvector method is used to investigate the critical point $(0,0)$ of the linear system

$$\begin{bmatrix} x' \\ y' \end{bmatrix} = \begin{bmatrix} a & b \\ c & d \end{bmatrix} \begin{bmatrix} x \\ y \end{bmatrix} \quad (4)$$

with the constant-coefficient matrix, A. The solutions for the characteristic equation are eigenvalues $\lambda_1$and λ_2.

$$det(A-\lambda I)=\begin{bmatrix} a-\lambda & b \\ c & d-\lambda \end{bmatrix}=(a-\lambda)(d-\lambda)-bc=0 \tag{5}$$

It is assumed that system's (5) isolated critical point is $(0,0)$. It implies that the determinant coefficient is nonzero for $ad-bc$ of the system $ax+by=0, cx+dy=0$. Therefore, $\lambda=0$ is not a solution of the system (4), and both eigenvalues of matrix A are nonzero. Table 1 below shows the type of critical point based on eigenvalues. Meanwhile, Theorem 1 is applied to examine the stability of equilibrium points.

Table 1: Type of critical point

Eigenvalues of A	**Type of Critical Point**
Real, unequal, same sign	Improper node
Real, unequal, opposite sign	Saddle point
Real and equal	Proper or improper node
Complex conjugate	Spiral point
Pure imaginary	Center

Theorem 1. *Let λ_1 and λ_2 be the eigenvalues of the system of the coefficient matrix A of the two-dimensional linear system* [17]

$$\frac{dx}{dt}=ax+by, \qquad \frac{dy}{dt}=cx+dy \tag{6}$$

with $ad-bc\neq 0$. Then, the system of the critical point $(0,0)$ is

1. Asymptotically stable if the real parts of λ_1 and λ_2 are both negative.
2. Stable if the real parts of λ_1 and λ_2 are both zero.
3. Unstable if either λ_1 or λ_2 has positive real part.

4. Results and discussion

4.1. Stability of equilibrium points

Based on the mathematical model in equation (2), the Jacobian Matrix obtained is

$$J=\begin{bmatrix} r-\frac{2rP}{K}-\alpha Z & -\alpha P \\ \beta Z-\frac{\theta Z}{\gamma+P}+\frac{P\theta Z}{(\gamma+P)^2} & \beta P-\mu-\frac{\theta P}{\gamma+P} \end{bmatrix} \tag{7}$$

System (2) has the following nonnegative equilibria, namely a trivial equilibrium $E_0(0,0)$, an axial equilibrium $E_1(K,0)$, and the interior equilibrium $E^*(P^*,Z^*)$ where

$$P^*=\frac{-(\beta\gamma-\mu-\theta)+\sqrt{(\beta\gamma-\mu-\theta)^2+4\beta\mu\gamma}}{2\beta} \tag{8}$$

$$Z^* = \frac{r}{\alpha}\left(1 - \frac{P^*}{K}\right) \tag{9}$$

4.1.1 The Stability of $E_0(0,0)$

The Jacobian Matrix around $E_0(0,0)$ is

$$J(E_0) = \begin{bmatrix} r & 0 \\ 0 & -\mu \end{bmatrix} \tag{10}$$

and the characteristic equation is computed as follow

$$(r - \lambda)(-\mu - \lambda) = 0 \tag{11}$$

Therefore,

$$\lambda_1 = r \qquad \lambda_2 = -\mu$$

From Theorem 1, the equilibrium point $E_0(0,0)$ is unstable since one of the eigenvalues obtained is positive integer. Hence, the algal bloom will not happen.

4.1.2 The Stability of $E_1(K, 0)$

The Jacobian Matrix and the characteristic equation is

$$J(E_1) = \begin{bmatrix} -r & -\alpha K \\ 0 & \beta K - \mu - \frac{\theta K}{\gamma + K} \end{bmatrix}$$

$$(-r - \lambda)\left(\beta K - \mu - \frac{\theta K}{\gamma + K} - \lambda\right) = 0 \tag{12}$$

and the eigenvalues are

$$\lambda_1 = r - \frac{2r}{K} \qquad \lambda_2 = \frac{\beta K\gamma + \beta K^2 - \mu\gamma - \mu K - \theta K}{\gamma + K}$$

Based on Theorem 1, $E_1(K, 0)$ is asymptotically stable if both eigenvalues have negative real parts. Therefore, in order for HAB to occur, the second eigenvalue must satisfy the following condition

$$\frac{(\beta K - \mu)(\gamma + K)}{K} < \theta$$

4.1.3 The Stability of $E^*(P^*, Z^*)$

The Jacobian Matrix is

$$J(E^*) = \begin{bmatrix} C_1 & -\alpha P^* \\ C_3 & C_2 \end{bmatrix} \tag{13}$$

where

$$C_1 = r - \frac{2rP^*}{K} - \alpha Z^*,$$

$$C_2 = \beta P^* - \mu - \frac{\theta P^*}{\gamma + P^*},$$

$$C_3 = \beta Z^* - \frac{\theta Z^*}{\gamma + P^*} + \frac{P^*\theta Z^*}{(\gamma + P^*)^2}.$$

The characteristic equation of E^* can be written as

$$(C_1 - \lambda)(C_2 - \lambda) - (-\alpha P^*)(C_3) = 0,$$

and the eigenvalues are

$$\lambda_1 = \frac{1}{2}\left(C_1 + C_2 - \sqrt{{C_1}^2 - 2C_1C_2 + {C_2}^2 - 4C_3P^*\alpha}\right),$$

$$\lambda_2 = \frac{1}{2}\left(C_1 + C_2 + \sqrt{{C_1}^2 - 2C_1C_2 + {C_2}^2 - 4C_3P^*\alpha}\right).$$

A system is stable if all eigenvalues are negative real parts. Thus, all the eigenvalues must satisfy the following conditions

$$C_1 + C_2 < \sqrt{{C_1}^2 - 2C_1C_2 + {C_2}^2 - 4C_3P^*\alpha},$$

$$-(C_1 + C_2) < \sqrt{{C_1}^2 - 2C_1C_2 + {C_2}^2 - 4C_3P^*\alpha}.$$

4.2 Numerical Solution

In this section, a set of parameter values (see Table 2) from [18] is used to substantiate analytical results obtained through numerical simulation.

Table 2: The abbreviations, default values and ranges of the parameters

Parameters	Symbols	Default values	Reported Ranges
Growth rate of phytoplankton population	r	0.0083 (hr^{-1})	0.00292-0.0117 (hr^{-1})
Environmental carrying capacity	K	1.667 $(\mathrm{g\,C\,m}^{-3})$	-
Grazing efficiency of zooplankton population	α	0.0375 $(\mathrm{m}^3\mathrm{g}^{-1}\mathrm{C}^{-1}\mathrm{hr}^{-1})$	0.025-0.0583 $(\mathrm{m}^3\mathrm{g}^{-1}\mathrm{C}^{-1}\mathrm{hr}^{-1})$
Growth efficiency of zooplankton population	β	0.0125 $(\mathrm{m}^3\mathrm{g}^{-1}\mathrm{C}^{-1}\mathrm{hr}^{-1})$	0.0083-0.0208 $(\mathrm{m}^3\mathrm{g}^{-1}\mathrm{C}^{-1}\mathrm{hr}^{-1})$
Higher predation on Z or natural death rate	μ	0.00083 (hr^{-1})	0.000625-0.00625 (hr^{-1})
Zooplankton grazing half saturation coefficient	γ	0.0025 $(\mathrm{g\,C\,m}^{-3})$	0.00083-0.00417 $(\mathrm{g\,C\,m}^{-3})$
Toxin production rate	θ	0.167 (hr^{-1})	-

4.2.1 Phase Portrait of Phytoplankton-Zooplankton

Based on the phase portrait in Figure 1, the trajectory of the population of phytoplankton and zooplankton are decreases rapidly. The curve is then converging to 0 indicating that $E_1(K,0)$ has reached a stable equilibrium point.

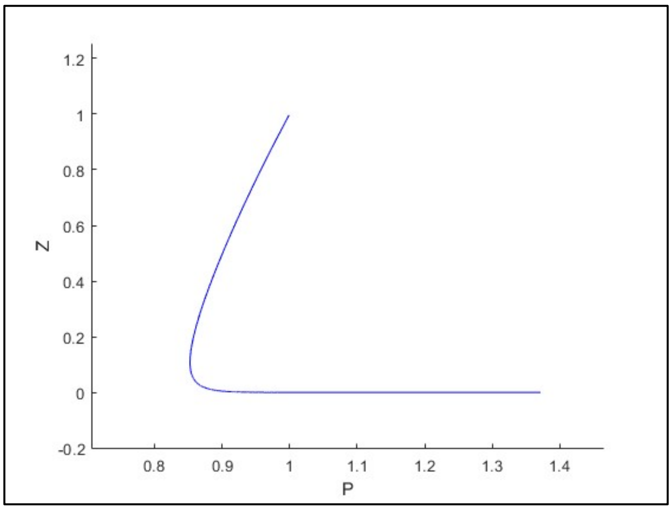

Figure 1 Phase Portrait of Phytoplankton Zooplankton

4.2.2 Phytoplankton-Zooplankton Model

Figure 2 shows the population changes of phytoplankton and zooplankton over time. The phytoplankton population increases due to favorable conditions but then drops to 0.8543 as resources get depleted. This decrease reduces predation pressure, allowing the phytoplankton to recover. Meanwhile, the zooplankton population declines over time, likely because of toxins released by the TPP that harm them.

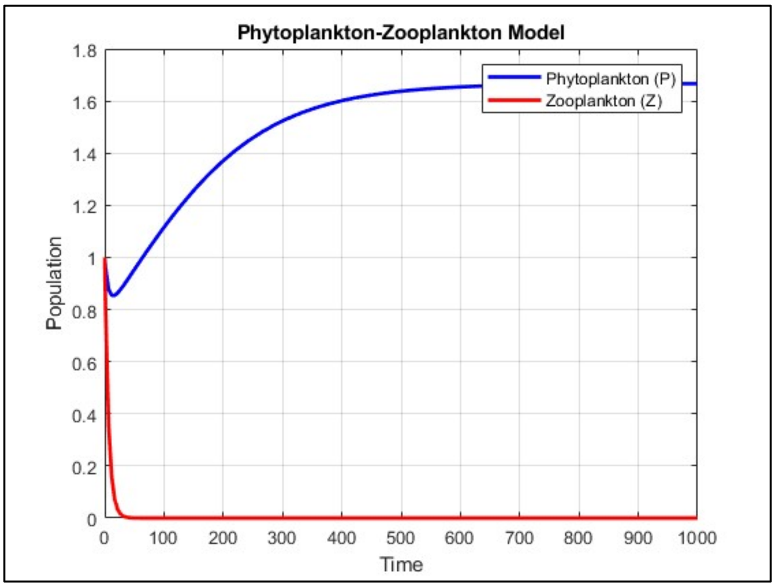

Figure 2 Phytoplankton-Zooplankton Population

4.2.3 Effect of Environmental Carrying Capacity

Figure 3 shows the stability between phytoplankton (P) and environmental carrying capacity (K). A bifurcation occurs at the branching point (BP), where the system initially exhibits stable as it approaches K =13.4239. However, beyond this point, the system changes from stable to a neutral saddle equilibrium (H) resulting instability at K =14.088. In this unstable region, no bifurcation occur until the end of the curve.

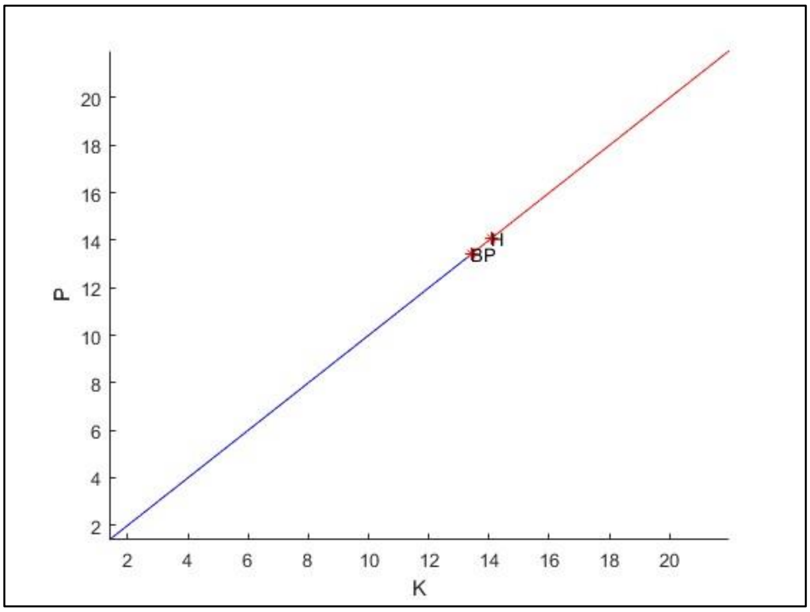

Figure 3 Effect of Environmental Carrying Capacity

Conclusion

From the results, it can be seen that the existence of toxin phytoplankton harm the population of zooplankton over time until it becomes 0. Meanwhile, the phytoplankton population drops only at the beginning, which decrease to 0.8543 as it starts to deplete the available resources. Moreover, it is evident that a bifurcation occurs when studying the stability between phytoplankton (P) and environmental carrying capacity (K) which at point K =13.4239. This situation is referred as Harmful Algal Blooms (HABs). From the modelling above, it gives better understanding about the occurrence of HABs event.

Acknowledgement

I would like to thank all people who have supported in completing this research.

References

[1] McPartlin, D. A., Loftus, J. H., Crawley, A. S., Silke, J., Murphy, C. S., & O'Kennedy, R. J. (2017). Biosensors for the monitoring of harmful algal blooms. In *Current Opinion in Biotechnology* (Vol. 45, pp. 164–169). Elsevier Ltd. https://doi.org/10.1016/j.copbio.2017.02.018

[2] Park, J., Kim, Y., Kim, M., & Lee, W. H. (2019). A novel method for cell counting of microcystis colonies in water resources using a digital imaging flow cytometer and microscope. *Environmental Engineering Research*, *24*(3), 397–403. https://doi.org/10.4491/EER.2018.266

[3] Yussof, F. N., Maan, N., & Md Reba, M. N. (2021). LSTM Networks to Improve the Prediction of Harmful Algal Blooms in the West Coast of Sabah. *International Journal of Environmental Research and Public Health*, *18*(14), 7650. https://doi.org/10.3390/ijerph18147650

[4] Jipanin, S. J., Muhamad Shaleh, S. R., Lim, P. T., Leaw, C. P., & Mustapha, S. (2019). The Monitoring of Harmful Algae Blooms in Sabah, Malaysia. *Journal of Physics: Conference Series*, *1358*(1). https://doi.org/10.1088/1742-6596/1358/1/012014

[5] Lim, P. T., Gires, U., & Leaw, C. P. (2012). Harmful algal blooms in Malaysian waters. Sains Malaysiana, 41(12), 1509–1515. https://www.ukm.my/jsm/pdf_files/SM-PDF-41-12-2012/03%20Lim.pdf

[6] Anton, A., Teoh, P. L., Mohd-Shaleh, S. R., & Mohammad-Noor, N. (2008). First occurrence of Cochlodinium blooms in Sabah, Malaysia. *Harmful Algae*, *7*(3), 331–336. https://doi.org/10.1016/j.hal.2007.12.013

[7] Michalak, A. M., Anderson, E. J., Beletsky, D., Boland, S., Bosch, N. S., Bridgeman, T. B., Chaffin, J. D., Cho, K., Confesor, R., Daloglu, I., DePinto, J. V., Evans, M. A., Fahnenstiel, G. L., He, L., Ho, J. C., Jenkins, L., Johengen, T. H., Kuo, K. C., LaPorte, E., … Zagorski, M. A. (2013). Record-setting algal bloom in Lake Erie caused by agricultural and meteorological trends consistent with expected future conditions. *Proceedings of the National Academy of Sciences of the United States of America*, *110*(16), 6448–6452. https://doi.org/10.1073/pnas.1216006110

[8] Hallegraeff, G. M. (1993). A review of harmful algal blooms and their apparent global increase. *Phycologia*, *32*(2), 79–99. https://doi.org/10.2216/i0031-8884-32-2-79.1

[9] Lemaire, V., Brusciotti, S., van Gremberghe, I., Vyverman, W., Vanoverbeke, J., & De Meester, L. (2012). Genotype×genotype interactions between the toxic cyanobacterium Microcystis and its grazer, the waterflea Daphnia. *Evolutionary Applications*, *5*(2), 168–182. https://doi.org/10.1111/j.1752-4571.2011.00225.x

[10] Sellner, K. G., Doucette, G. J., & Kirkpatrick, G. J. (2003). Harmful algal blooms: Causes, impacts and detection. In *Journal of Industrial Microbiology and Biotechnology* (Vol. 30, Issue 7, pp. 383–406). https://doi.org/10.1007/s10295-003-0074-9

[11] Schaeffer, B. A., Iiames, J., Dwyer, J., Urquhart, E., Salls, W., Rover, J., & Seegers, B. (2018). An initial validation of Landsat 5 and 7 derived surface water temperature for U.S. lakes, reservoirs, and estuaries. *International Journal of Remote Sensing*, *39*(22), 7789–7805. https://doi.org/10.1080/01431161.2018.1471545

[12] Sidabutar, T., Srimariana, E. S., Cappenberg, H. A. W., & Wouthuyzen, S. (2022). Harmful algal bloom of the three selected coastal bays in Indonesia. *IOP Conference Series: Earth and Environmental Science*, *1119*(1). https://doi.org/10.1088/1755-1315/1119/1/012035

[13] Masó, M., & Garcés, E. (2006). Harmful microalgae blooms (HAB); problematic and conditions that induce them. *Marine Pollution Bulletin*, *53*(10–12), 620–630. https://doi.org/10.1016/j.marpolbul.2006.08.006

[14] Wikan, A., & Kristensen, Ø. (2019). Prey-Predator Interactions in Two and Three Species Population Models. *Discrete Dynamics in Nature and Society*, *2019*, 1–14. https://doi.org/10.1155/2019/9543139

[15] Chen, S., Dobramysl, U., & Täuber, U. C. (2018). Evolutionary dynamics and competition stabilize three-species predator–prey communities. *Ecological Complexity*, *36*, 57–72. https://doi.org/10.1016/j.ecocom.2018.05.003

[16] Holling, C. S. (1959). Some Characteristics of Simple Types of Predation and Parasitism. *The Canadian Entomologist*, *91*(7), 385–398. https://doi.org/10.4039/Ent91385-7

[17] Yang Kuang. (1993). *Delay Differential Equations: With Applications in Population Dynamics*. Academic Press. New York.

[18] Edwars,A. (1999). Zooplankton Mortality and the Dynamical Behavior of Plankton Population Models. *Bulletin of Mathematical Biology, 61(2),* 303-339. https//doi.org/10.1006/bulm.1998.0082